Structures of *Escherichia coli* Histidinol-Phosphate Aminotransferase and Its Complexes with Histidinol-Phosphate and *N*-(5′-Phosphopyridoxyl)-L-Glutamate: Double Substrate Recognition of the Enzyme[†,‡]

Kazuki Haruyama,[§] Tadashi Nakai,[§,||] Ikuko Miyahara,[§] Ken Hirotsu,*[,§] Hiroyuki Mizuguchi,[⊥] Hideyuki Hayashi,[⊥] and Hiroyuki Kagamiyama[⊥]

Department of Chemistry, Graduate School of Science, Osaka City University, Sugimoto, Sumiyoshi-ku, Osaka 558-8585, Japan, and Department of Biochemistry, Osaka Medical College, Takatsuki, Osaka 569-8686, Japan

Received December 6, 2000

ABSTRACT: Histidinol-phosphate aminotransferase (HspAT) is a key enzyme on the histidine biosynthetic pathway. HspAT catalyzes the transfer of the amino group of L-histidinol phosphate (Hsp) to 2-oxoglutarate to form imidazole acetol phosphate (IAP) and glutamate. Thus, HspAT recognizes two kinds of substrates, Hsp and glutamate (double substrate recognition). The crystal structures of native HspAT and its complexes with Hsp and *N*-(5′-phosphopyridoxyl)-L-glutamate have been solved and refined to *R*-factors of 19.7, 19.1, and 17.8% at 2.0, 2.2, and 2.3 Å resolution, respectively. The enzyme is a homodimer, and the polypeptide chain of the subunit is folded into one arm, one small domain, and one large domain. Aspartate aminotransferases (AspATs) from many species were classified into aminotransferase subgroups Ia and Ib. The primary sequence of HspAT is less than 18% identical to those of *Escherichia coli* AspAT of subgroup Ia and *Thermus thermophilus* HB8 AspAT of subgroup Ib. The X-ray analysis of HspAT showed that the overall structure is significantly similar to that of AspAT of subgroup Ib rather than subgroup Ia, and the N-terminal region moves close to the active site like that of subgroup Ib AspAT upon binding of Hsp. The folding of the main-chain atoms in the active site is conserved between HspAT and the AspATs, and more than 40% of the active-site residues is also conserved. The eHspAT recognizes both Hsp and glutamate by utilizing essentially the same active-site folding as that of AspAT, conserving the essential residues for transamination reaction, and replacing and relocating some of the active-site residues. The binding sites for the phosphate and the α-carboxylate groups of the substrates are roughly located at the same position and those for the imidazole and γ-carboxylate groups at the different positions. The mechanism for the double substrate recognition observed in eHspAT is in contrast to that in aromatic amino acid aminotransferase, where the recognition site for the side chain of the acidic amino acid is formed at the same position as that for the side chain of aromatic amino acids by large-scale rearrangements of the hydrogen bond networks.

Aminotransferase, which requires a pyridoxal 5′-phosphate (PLP)[1] as a cofactor, reversibly catalyzes the transamination reaction, which plays an important role in amino acid metabolism (*1*). The PLP of the aminotransferase takes up the α-amino group of an amino acid 1 to give a pyridoxamine 5′-phosphate (PMP) and 2-oxo acid of the amino acid. Next, the amino group of PMP is transferred to 2-oxoglutarate to yield glutamate and regenerate PLP. Thus, the overall transamination reaction consists of essentially the same two-half transamination reactions (Scheme 1).

Scheme 1

PLP-enzyme + α-amino acid 1 ⇌ PMP-enzyme + 2−oxo acid (1)

PMP-enzyme + 2-oxoglutarate ⇌ PLP-enzyme + glutamate (2)

An aminotransferase has its own α-amino acid 1 in reaction 1 of Scheme 1 as the substrate and a common amino acid, glutamate in reaction 2. In an aromatic amino acid and a branched chain amino acid aminotransferase, an α-amino acid 1 is aromatic amino acids and hydrophobic amino acids, respectively. An aminotransferase has to be able to select and bind two kinds of amino acids, the side chains of which are different in shape and property, from many other small molecules. The double substrate recognition essential for the

[†] This study was supported by a Research Grant from the Japan Society for the Promotion of Science (Research for the Future), and by a Grants-in-Aid for Scientific Research on Priority Areas from the Ministry of Education, Science, Sports and Culture of Japan (12020249).

[‡] Coordinates for eHspAT and its complexes with histidinol-phosphate and *N*-(5′-phosphopyridoxyl)-L-glutamate have been deposited in the RSCB Protein Data Bank as entries 1GEW, 1GEX, and 1GEY, respectively.

* To whom correspondence should be addressed. E-mail: hirotsu@sci.osaka-cu.ac.jp. Fax: +81-6-6605-3131.

[§] Osaka City University.

[||] Present address: RIKEN Harima Institute, 1-1-1 Kouto, Mikazuki, Sayo-gun, Hyogo 679-5148.

[⊥] Osaka Medical College.

[1] Abbreviations: PLP, pyridoxal 5′-phosphate; PMP, pyridoxamine 5′-phosphate; AspAT, aspartate aminotransferase; eAspAT, *Escherichia coli* AspAT; tAspAT, *Thermus thermophilus* HB8 AspAT; cAspAT, pig cytosolic AspAT; HspAT, histidinol-phosphate aminotransferase; eHspAT, *Escherichia coli* HspAT; Hsp, L-histidinol phosphate; IAP, imidazole acetol phosphate; Pxy−Glu, *N*-(5′-phosphopyridoxyl)-L-glutamate; ASA, accessible surface area; MIR, multiple isomorphous replacement; rms, root-mean-square; Tyr70*, the asterisk (*) indicates a residue from another subunit of the dimer unit.

10.1021/bi002769u CCC: $20.00
Published on Web 03/24/2001

Scheme 2

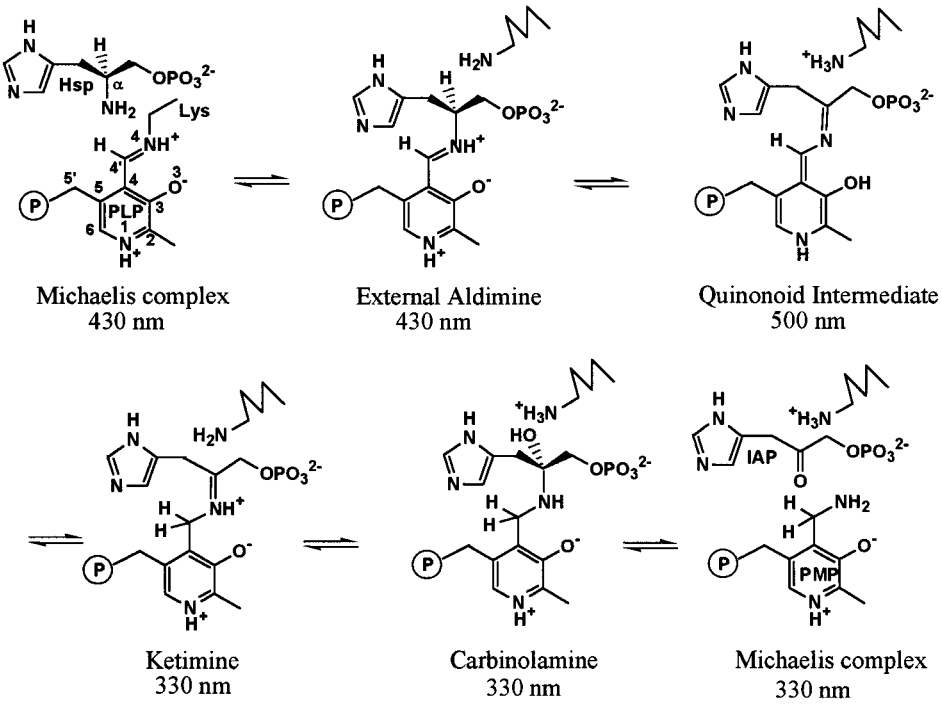

transamination reaction requires an ingenious design of the active-site structure in comparison with a single substrate recognition. The X-ray crystallographic studies of a hexamutant of *Escherichia coli* aspartate aminotransferase (eAspAT) and *Paracoccus denitrificans* aromatic amino acid aminotransferase showed that binding sites for both acidic and aromatic side chains of the substrate are formed at the same location by the rearrangement of the hydrogen bond network of the active site without a conformational change in the backbone structure of the enzymes (*2*, *3*).

Histidinol-phosphate aminotransferase (HspAT) catalyzes the transfer of the amino group of the L-histidinol phosphate (Hsp) to 2-oxoglutarate to form imidazole acetol phosphate (IAP) and glutamate. HspAT is a product of the third structural gene (*hisC*) of the histidine operon associated with the histidine biosynthetic pathway, which is a key and common metabolic pathway (*4*, *5*). The enzyme consists of two identical subunits, and each subunit is composed of 356 amino acid residues with a subunit molecular weight of 39 315 and binds a PLP. The reaction process of eHspAT with Hsp is given in Scheme 2 based on the proposed mechanism of the transamination reaction (*6*, *7*). Hsp binds to eHspAT in the PLP form to make a new Schiff base linkage with PLP. The amino group of the released Lys eliminates the α-proton to give the quinonoide intermediate. The protonated amino group of Lys adds an α-proton to C4′ to produce the ketimine. The ketimine is hydrolyzed to PMP and IAP through the carbinolamine. Since the Hsp is not amino acid but amine, not only the side-chain part (imidazole ring), but also the α-carboxylate part (phosphate) is different from the corresponding groups of glutamate. The enzyme should have the mechanism switching the binding site for the basic side-chain of Hsp to that for the acidic side-chain of glutamate. Moreover, the bulky phosphate group with double negative charge and the carboxylate group with a single negative charge must be accommodated in the same region of the active site.

HspAT is homologous to AspATs (*8*), which have been extensively studied using biochemical, spectroscopic, and X-ray crystallographic methods (*9*−*16*). AspATs were classified into the aminotransferase subgroup I (*17*), which was further subdivided into subgroups Ia and Ib (*18*). More than 40% amino acid sequence identities were observed in each group (*19*), but less than 16% sequence identities between them. Despite the low sequence identities between the AspATs of subgroups Ia and Ib, the overall and active-site structures are apparently similar. However, there are two distinct differences between them. In AspAT subgroup Ia, Arg292 recognizes the side-chain carboxylate of the substrate, while in AspAT subgroup Ib, Lys109 forms a salt bridge with the side-chain carboxylate. In AspAT subgroup Ia, substrate binding induces a large movement of the small domain as a whole to close the active site, but in the enzyme of subgroup Ib, only the N-terminal region approaches the active site.

The aligned amino acid sequences of *E. coli* HspAT (eHspAT), eAspAT of subgroup Ia, and *Thermus thermophilus* HB8 AspAT (tAspAT) of subgroup Ib show that sequence identities of eHspAT with respect to eAspAT and tAspAT are 18.5 and 17.4%, respectively (*20*), and some of the important residues for catalytic action in the active site do not seem to be conserved among the enzymes. The overall structure of eHspAT is expected to be similar to those of eAspAT of subgroup Ia and tAspAT of subgroup Ib, but the precise three-dimensional structure of eHspAT is unknown. AspATs bind and catalyze only acidic amino acids (aspartate and glutamate), while eHspAT recognizes Hsp and glutamate as substrates, although eHspAT is homologous to AspATs. It is interesting to elucidate the mechanism to recognize double substrates (Hsp and glutamate) which are different in shapes, sizes, charges, and properties and to compare the mechanism observed in eHspAT with that in the aromatic amino acid aminotransferase.

Structure determination of eHspAT should help in understanding the double substrate recognition, the role of the active-site residues, and the reaction mechanism of the aminotransferases, and comparing the three-dimensional structures between eHspAT and AspATs of subgroups Ia and Ib provides some insight into the evolutionary relationships of the PLP-dependent enzymes. Here we report the X-ray crystallographic studies of eHspAT in the unliganded form, eHspAT complexed with Hsp and eHspAT complexed with *N*-(5′-phosphopyridoxyl)-L-glutamate (Pxy−Glu) at 2.0 and 2.2 and 2.3 Å resolution, respectively.

MATERIALS AND METHODS

Preparation of eHspAT in the Complex with Pxy-Glu. Pxy−Glu was synthesized according to the method reported by Severin (*21*). To obtain apoenzyme, the PLP form of enzyme (20−25 mg/mL) was treated with 10 mM glutamate and 1.0 M potassium phosphate (pH 7.0) for 12 h at 25 °C. The solution was dialyzed overnight against 500 mL of 100 mM Tris-HCl, pH 7.7, with three exchanges of buffer. The glutamate and dissociated PMP were washed out with the same buffer using centripep YM-30. To this apoenzyme, Pxy−Glu was added to a 10-fold concentration and was incubated 12 h at 25 °C to obtain holoenzyme.

Protein Expression, Purification, and Crystallization. The *Nde*I site was built into plasmid pUC118 at the initiation codon ATG of the *lac*Z gene by a site-directed mutagenesis. The PCR-cloned structural gene of eHspAT has been inserted between *Eco*RI and the *Nde*I restriction site of the mutated pUC118. *E. coli* HB101 was transformed with the resultant plasmid, pUC118-*hisC*. The enzyme was purified by a three-step column chromatography procedure: first by a DEAE-Toyopearl column (Tosoh) with a linear gradient from 0 to 0.3 M NaCl, followed by a Gigapite column (Seikagaku Kogyo) using a linear gradient of pottasium phosphate (5−150 mM) and a phenyl-Sepharose Cl-4B column (Pharmacia) using a linear gradient of 25 to 0% saturated ammonium sulfate. Selenomethionyl eHspAT was prepared by overexpressing pUC118-*hisC* in *E. coli* DL41(*metA*$^-$) cells grown in a synthetic medium containing DL-selenomethionine in place of methionine (*22*). The selenomethionyl protein was purified and crystallized in the same way as the wild-type one.

Crystallization for the native enzyme in the PLP form was carried out at 20 °C using the hanging-drop vapor-diffusion method, using 20−25 mg/mL protein solution and 21% (w/v) PEG 4000, 200 mM $MgCl_2$, 100 mM Tris-HCl, pH 7.7, as the reservoir solution. After 30−50 h, crystals had grown to dimensions of about 0.3 × 0.3 × 0.4 mm. Crystallization of HspAT in the complex with Hsp was performed using the hanging-drop vapor-diffusion method in combination with microseeding, using 20−25 mg/mL protein solution and 17.5% (w/v) PEG 4000, 82 mM Hsp, 200 mM $MgCl_2$, 100 mM Tris-HCl, pH 7.7, as the reservoir solution. When an excess amount of the substrate Hsp was added to the protein solution, the solution changed from yellow to colorless and the complex of eHspAT·Hsp was obtained as colorless crystals. Crystals of Pxy−Glu complex were obtained using the same procedure as that for the native enzyme. A preliminary X-ray study of the native enzyme, HspAT·Hsp and Pxy−Glu complex indicated that these three crystals are isomorphous.

Data Collection. An X-ray diffraction data set for a native crystal was collected to a 2.0 Å resolution at 293 K on a Rigaku R-AXIS IIc imaging plate detector using monochromated CuKα radiation (40 kv, 100 mA). The space group is *C*2 with cell dimensions of $a = 133.3$, $b = 63.8$, $c = 46.2$ Å, and $\beta = 104.1°$. There is one subunit in the asymmetric unit, and approximately 50.4% of the crystal volume is occupied by solvent. The data sets for the eHspAT·Hsp crystal, eHspAT·Pxy−Glu crystal, a selenomethionyl protein crystal, and crystals soaked in 1mM C_2H_5HgCl were collected to 2.2, 2.3, 2.1, and 3.1 Å resolution, respectively, at 293 K with a Rigaku R-AXIS IIc. All data were processed and scaled using the programs DENZO and SCALEPACK (*23*) (Table 1).

Structure Determination. The structure of the native eHspAT in the PLP form was solved by the MIR method, using two isomorphous data sets. The scaling of all data and map calculations were performed with the CCP4 program suite (*24*). The difference Patterson map calculation for ethylmercury chloride using the data from 8 to 3.1 Å resolution allowed a clear interpretation of one mercury site. The positions of three selenium sites in the selenomethionyl eHspAT were determined from the difference Fourier map based on the mercury phasing. Refinement of the heavy atom parameters and calculation of the initial phases were performed with the program MLPHARE (*24*). The resulting MIR map has a mean figure-of-merit of 0.33 at a resolution of 10−3.0 Å. The map was significantly improved by the process of solvent flattening (*25*) and histogram matching (*26*) with the program DM (*24*). The mean figure-of-merit reached 0.78 with the same resolution range. The map was of good quality and the model of the subunit was gradually built into the 3.0 Å map through several cycles of model building using the program O (*27*).

The structure of eHspAT was refined by simulated annealing and energy minimization using the program X-PLOR (*28*, *29*), using X-ray data from 8.0−2.5 Å resolution. The entire structure including the PLP molecule was scrutinized by successively omitting 10 residue segments of the model from the phasing calculation and inspecting the map. Refinement by simulated annealing and rebuilding was alternated until no further improvements in the structure and statistics were apparent with the R_{factor} of 21.8% and R_{free} of 26.6%. The resolution was progressively increased to 2.0 Å and after several rounds of refinement and manual rebuilding, R_{factor} and R_{free} were reduced to 24.2 and 27.7%, respectively. Water molecules were picked up on the basis of the peak heights and distance criteria from the difference map. The water molecules whose thermal factors were above 52 Å^2 (maximum thermal factor of the main chain) after refinement were removed from the list. Further model building and refinement cycles resulted in an R_{factor} of 19.7% and R_{free} of 24.7%, using 24 041 reflections [$F_o > 2\sigma(F_o)$] between 8.0 and 2.0 Å resolution (Table 1). During the last step of the refinement, unambiguous water molecules were added including those with a temperature factor higher than 52 Å^2. The maximum temperature factor of the water molecules was 70 Å^2.

The refinement of eHspAT in the complex with Hsp was started using the coordinates of the unliganded eHspAT except for PLP as an initial model. The structure of eHspAT was refined by simulated annealing and energy minimization

Table 1: Data Collection, MIR, and Refinement Statistics

crystal	native	Hsp	Pxy-Glu	Se-Met	EMC[e]
diffraction data					
resolution (Å)	2.0	2.2	2.3	2.1	3.1
no. of reflections					
unique	25 542	18 942	16 231	21 597	6724
observed	88 073	87 507	55 982		
completeness (%)	96.7 (85.6)[d]	98.3 (95.5)[d]	97.8 (97.4)	95.7	97.2
R_{merge} (%)[a]	6.9 (23.0)[d]	8.6 (23.1)[d]	8.9 (26.5)	8.8	13.7
MIR					
R_{diff} (%)[b]				11.2	13.1
phasing power [c]				0.5	0.4
no. of sites				3	1
refinement					
resolution limits (Å)	8.0−2.0	8.0−2.2	8.0−2.3		
R_{factor} (%)	19.7 (31.2)[d]	19.1 (28.5)[d]	17.8 (24.0)[d]		
R_{free} (%)	24.7 (33.2)[d]	26.1 (33.5)[d]	25.7 (34.9)[d]		
deviations					
bond lengths (Å)	0.008	0.008	0.006		
bond angles (deg)	1.4	1.4	1.3		
mean *B* factors					
main chain atoms (Å^2)	21.6	22.6			
side-chain atoms (Å^2)	24.0	23.9			
cofactor atoms (Å^2)	16.8	20.2			
water atoms (Å^2)	34.6	31.8			

[a] $R_{merge} = \sum_{hkl} \sum_i |I_{hkl,i} - \langle I_{hkl}\rangle| / \sum_{hkl} \sum_i I_{hkl,i}$, where I = observed intensity and $\langle I\rangle$ = average intensity for multiple measurements. [b] $R_{diff} = \sum||F_{PH}| - |F_P||/\sum|F_P|$, where $|F_{PH}|$ and $|F_P|$ are the derivative and native structure-factor amplitudes, respectively. [c] Phasing power is the ratio of the root-mean-square (rms) of the heavy atom scattering amplitude and the lack of closure error. [d] The values in the parentheses are for highest resolution shells (2.07−2.00 Å) in the native enzyme, (2.28−2.20 Å) in the Hsp complex, and (2.38−2.30 Å) in the Pxy−Glu complex. [e] Ethylmercury chlorode.

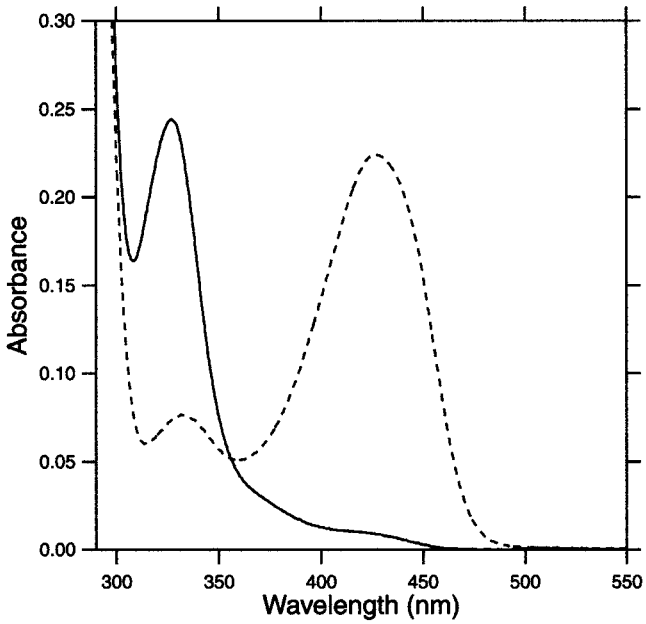

FIGURE 1: Absorption spectra of wild-type HspAT in the absence (broken line) and the presence of substrate Hsp at pH 7.7 and 25 °C with light path of 1 mm; 25 mg/mL protein in 17.5% (w/v) PEG 4000, 200 mM $MgCl_2$, 100 mM Tris-HCl, pH 7.7; 82 mM Hsp.

(*28*, *29*) using X-ray data from 8.0−2.2 Å resolution. When the R_{factor} was below 25%, the difference Fourier map clearly exhibited the residual electron density corresponding to the substrate Hsp and cofactor. The crystals were colorless, and the spectra showed the loss of the 430 nm absorption with a new absorption band at 330 nm when eHspAT was treated with Hsp (Figure 1). Thus, ketimine, carbinolamine, and the IAP·PMP forms shown in Scheme 1 were selected as the candidates for the Hsp−cofactor complex. The residual electron density of Hsp is connected to the N4 atom of the cofactor, indicating that Hsp is covalently bonded to the cofactor (Figure 5a). The Hsp−cofactor bond structure was then assumed to be ketimine or carbinolamine, which was modeled into the residual electron density. The ketimine form showed a good fit to the electron density, but the α-OH group of carbinolamine could not be fitted into the electron density. The Hsp−cofactor bond structure was then assigned to be ketimine as the most probable form. The water molecules whose thermal factors were above 59 Å^2 (maximum thermal factor of the main chain) after refinement were removed from the list. Further model building and refinement cycles resulted in an R_{factor} of 19.1% and R_{free} of 26.1% using 18 299 reflections [$F_o > 2\sigma(F_o)$] between 8.0 and 2.2 Å resolution (Table 1). During the last step of the refinement, unambiguous water molecules were added even when having a high-temperature factor. The maximum temperature factor of the water molecules was 73 Å^2.

The refinement of eHspAT in the complex with Pxy−Glu was started using the coordinates of the unliganded eHspAT except for PLP as an initial model. The structure of eHspAT·Pxy−Glu was refined by simulated annealing and energy minimization (*28*, *29*) using X-ray data from 8.0−2.3 Å resolution. When the R_{factor} was below 25%, the difference Fourier map clearly exhibited the residual electron density corresponding to the Pxy−Glu. The water molecules whose thermal factors were above 56 Å^2 (maximum thermal factor of the main chain except for that of Ala23 and Arg24) after refinement were removed from the list. Further model building and refinement cycles resulted in an R_{factor} of 17.8% and R_{free} of 25.7% using 16 008 reflections [$F_o > 2\sigma(F_o)$] between 8.0 and 2.3 Å resolution (Table 1). During the last step of the refinement, unambiguous water molecules were added even when having a high-temperature factor. The maximum temperature factor of the water molecules was 70 Å^2.

```
                10         20         30         40         50         60         70         80         90
cAspAT  APPSVFAEVP QAQPVLVFKL IADFRED..PDP RKVNLGVGAY RTDDCQPWVL PVVRKVEQRI ANNSSLNHEY LPILGLAEFR TCASRLALGD
eAspAT  ....MFENIT AAPADPILGL ADLFRAD..ERP GKINLGIGVY KDETGKTPVL TSVKKAEQYL LENE.TTKNY LGIDGIPEFG RCTQELLFGK
                        <--H1-->           <a'>                <-----H2----->              <----H3----->
tAspAT  .MRGLSRRVQ AMKPSATVAV NAKALELRRQGV DLVALTAGEP D.....FDTP EHVKEAARRA LAQ..GKTKY APPAGIPELR EALAEKFRRE
              <-H0->     <-----H1------>     <a'>                <----H2----->              <------H3------
eHspAT  MSTVTITDLA RENVRNLTPY QSARRLG...GN GDVWLNANEY P.....TAVE F.....QLTQ ..Q..TLNRY PEC.QPKAVI ENYAQYAG..
                     <H0>                  <a'>                                          <----H3---->
CONS                                 r     g    v L a ey         v               q      Y            e  a

                100        110        120        130        140        150        160        170        180
cAspAT  DSPALQEKRV GGVQSLGGTG ALRIGAEFLA RWYNGTNNKD TPVYVSSPTW ENHNGVFTTA GFKDIRSYRY WDTEKRGLDL QGFLSDLENA
eAspAT  GSALINDKRA RTAQTPGGTG ALRVAADFLA KNTSVK..R. ..VWVSNPSW PNHKSVFNSA GL.EVREYAY YDAENHTLDF DALINSLNEA
          <H4>   <--a--><-------H5------->      <---b---->     <--H6-->     <-c-->            <--H7--->
tAspAT  NG..LSVTPE ETIVTVGGKQ ALFNLFQAIL ..DPGD..E. ..VIVLSPYW VSYPEMVRFA GG.VVVEVET LPEEGFVP.. DPERVRRAIT
        >           <a-> <-----H5----->          <---b---->     <--H6-->     <-c-->              <H7->
eHspAT  ......VKPE QVLVSRGADE GIELLIRAFC .EPGKD..A. ..ILYCPPTY GMYSVSAETI GV.ECRTVPT L..DNWQL.. DLQGISDKLD
                  <a-> <-----H5----->          <--b--->       <--H6--->    <c->                <-H7->
CONS          v pe    v  G           a        d            P     y        G    r   t l      l   d

                190        200        210        220        230        240        250        260        270
cAspAT  PQFSIFVLHA CAHNPTGTDP TPEQWKQIAS VMKRRFLFPF FDSAYQGFAS GNLEKDAWAI RYFVSEGFEL FCAQSFSKNF GLYNERVGNL
eAspAT  QAGDVVLFHG CCHNPTGIDP TLEQWQTLAQ LSVEKGWLPL FDFAYQGFAR G.LEEDAEGL RAFAAMHKEL IVASSYSKNF GLYNERVGAC
        <d->                 <----H8-----><--e-->                <---H9---><--f-->                  <--g
tAspAT  PRTKALVVNS .PNNPTGAVY PKEVLEALAR LAVEHDFYLV SDEIYEHLLY E.GE.HFS.. .PGRVAPEHT LTVNGAAKAF AMTGWRIGYA
          <--d-->              <-----H8------>  <-e-->                          <--f-->                  <g-
eHspAT  G.VKVVYVCS .PNNPTGQLI NPQDFRTLLE LTR.GKAIVV ADEAYIEFCP Q.AS.LAG.. .WLAEY.PHL AILRTLSKAF ALAGLRCGFT
          <--d-->              <-----H8---->     <-e-->                          <--f-->                  <-g
CONS       k   v s  pnNPTG           l   l        v  DeaY  f          a            h        sKaF al g R G

                280        290        300        310        320        330        340        350        360
cAspAT  TVVAKEPDSI LRVLSQMQKI VRVTWSNPPA QGARIVARTL SDPELFHEWT GNVKTMADRI LSMRSELRAR LEALKTPGTW NHITDQIGMF
eAspAT  TLVAADSETV DRAFSQMKAA IRANYSNPPA HGASVVATIL SNDALRAIWE QELTDMRQRI QRMRQLFVNT LQEKGANRDF SFIIKQNGMF
        -->     <-----H11------>       <---H12---->   <---------------H13--------------->       <H14>    <
tAspAT  CG.......P KEVIKAMASV SSQSTTSPDT IAQWATLEAL TN...QEASR AFVEMAREAY RRRRDLLLEG LTALG....L KAVRPSGAFY
        >           <----H11---->       <----H12----->    <-------------H13-------------->              <
eHspAT  LA.......N EEVINLLMKV IA..PYPLST PVADIAAQAL S.....PQGI VAMRERVAQI IAEREYLIAA LKEIPC..VE QVFDS.ETNY
        ->          <-H11-->            <---H12--->       <------------H13------------>      <b''>       <
CONS                 evi     v          t       a al s                   i    R  l    L                   y

                  370        380                390        400        410
cAspAT  SFTGL......NPKQV EYLINEKHIY LLPS.........GRINMC GLTTKNLDYV ATSIHEAVTK IQ
eAspAT  SFSGL......TKEQV LRLREEFGVY AVAS.........GRVNVA GMTPDNMAPL CEAIVA.VL. ..
        b'>         <---H15---> <c'->           <d'>        <--H16--->
tAspAT  VLMDTSPIAPDEVRAA ERLLEA.GVA VVPGTDF.AAFGHVRLSYA TSEENLRKAL ERFARV.LGR A.
        b'->        <---H15--->   <-c'->        <d'->       <-----H16----->
eHspAT  ILARFK....ASSAVF KSLWDQ.GII LRDQNKQPSLSGCLRITV. GTREESQRVI DALRAE.QV. ..
        -b'->       <---H15----->  <-c'->        <d'->       <---H16--->
CONS     l                 L    g                R     g  e
```

FIGURE 2: Alignments of eHspAT, tAspAT, eAspAT, and pig cytosolic AspAT with secondary structures. α-Helices are indicated by H0−H16, and β-sheets by a−g in the large domain and a′−d′ in the small domain. eAspAT and pig cytosolic AspAT belong to aminotransferase subgroup Ia, and tAspAT belongs to subgroup Ib. In the consensus sequence, capital letters imply full conservation, and small letters imply conservation between eHspAT and one of two subgroups.

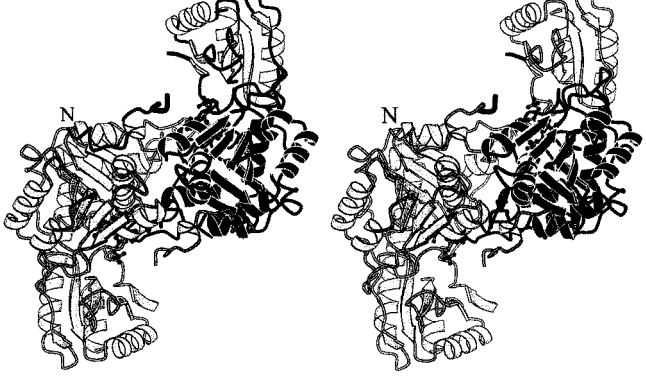

FIGURE 3: Cα ribbon tracing of the eHspAT in the complex with Hsp viewed down the molecular 2-fold axis. One subunit is represented by the shaded ribbon, and the small and large domains of the other subunit by the lightly shaded and full ribbons, respectively. Hsp−cofactor bond structure, shown by the ball-and stick model, is bound to the active-site pocket, which is located at the domain interface and the subunit interface.

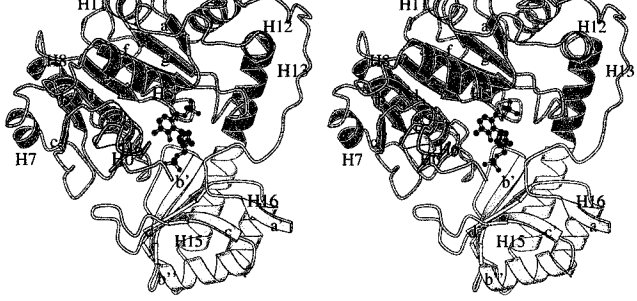

FIGURE 4: Stereoview of the subunit structure in eHspAT in the complex with Hsp with secondary structure assignment. α-Helices are denoted by H0−H16, and β-sheets by a−g in the large domain and a′−d′ in the small domain. The shaded and open ribbons represent the large and the small domains, respectively.

Spectrophotometric Measurement. The absorption spectra of the native eHspAT and eHspAT in the complex with Hsp were recorded with a Hitachi spectrophotometer, model 3300, using 1-mm cell, with the same protein and substrate concentration and buffer solution as that for crystallization. The free enzyme exhibited a 427 nm absorption band characteristic of the internal aldimine form of the enzyme. The enzyme treated with excess amount of Hsp resulted in a new band at 327 nm with the disappearance of 427 nm absorption (Figure 1)

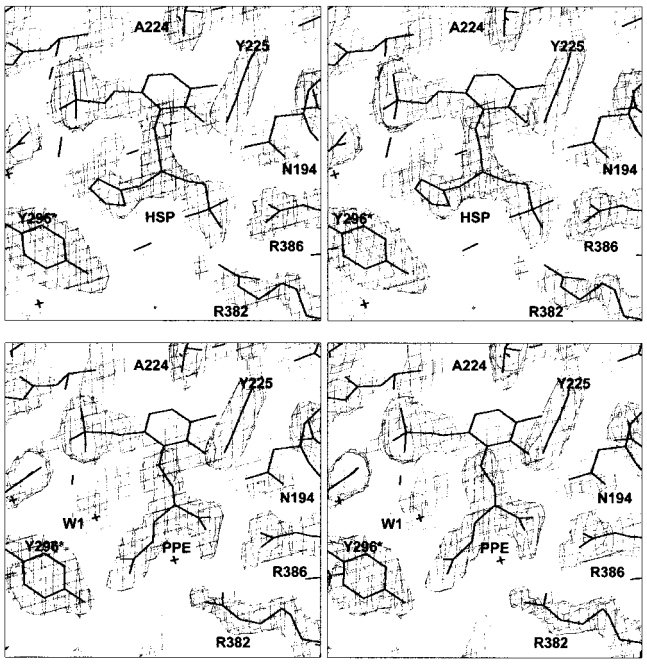

FIGURE 5: (a, top) Stereoview of the $2F_o - F_c$ electron density map calculated using 8.0 and 2.2 Å resolution for Hsp−cofactor complex. The electron density map clearly shows the formation of a covalent bond between Hsp and cofactor, and the absence of a hydroxy group on the α-carbon of Hsp, supporting the fact that the Hsp−cofactor complex is in the ketimine form. (b, bottom) Stereoview of the $2F_o - F_c$ electron density map calculated using 8.0 and 2.3 Å resolution for Pxy−Glu complex.

Quality of the Structure. The refined model of eHspAT contains 2594 non-hydrogen atoms and a covalently bound molecule of PLP. Additionally, 142 water molecules were included. The model lacks four N-terminal residues, Thr18 to Asp32, and five C-terminal residues. The average thermal factors of the main-chain atoms (N, Cα, C, and O) are 22 Å^2.

The refined model of eHspAT·Hsp contains 2641 non-hydrogen atoms and a covalently bound molecule of the cofactor in the ketimine form. Additionally, 120 water molecules were included. The model lacks four N-terminal residues, Ser22 to Asn30, and five C-terminal residues. The average thermal factors of the main-chain atoms (N, Cα, C, and O) are 23 Å^2.

The refined model of eHspAT·Pxy−Glu contains 2611 non-hydrogen atoms and a noncovalently bound Pxy−Glu. Additionally, 116 water molecules were included. The model lacks four N-terminal residues, Thr18 to Ser22, Arg25 to Asp32, and five C-terminal residues. The average thermal factors of the main-chain atoms (N, Cα, C, and O) are 21 Å^2.

Analysis of the stereochemistry with PROCHECK (*30*) showed that all the main-chain atoms fall within the additional allowed regions of the Ramachandran plot for all structures. The 265 and 28 residues of eHspAT are in the most favored region and the additionally allowed region, respectively, the 265 and 33 residues of eHspAT·Hsp are in the most favored region and the additionally allowed region, respectively, and the 262 and 31 residues of eHspAT·Pxy−Glu are in the most favored region and the additionally allowed region. Pro138, Pro192, and Pro195 assume cis conformations.

RESULTS AND DISCUSSION

Overall Structure. The structure of eHspAT was superimposed on that of tAspAT using the program DALI (*31*) to give an initial alignment, which was then manually modified to have the maximum agreement of the conserved residues between the two enzymes. The primary sequence alignment thus obtained was combined with the reported alignment among tAspAT, eAspAT, and pig cytosolic AspAT (*19*) (Figure 2). The residues are numbered according to the sequence of the pig cytosolic AspAT. The sequence identities of eHspAT with respect to tAspAT, eAspAT, and pig cytosolic AspAT are 17.9, 15.2, and 14.6%, respectively.

The overall structure of eHspAT is shown in Figure 3. The eHspAT is folded into a dimeric form with a crystallographic 2-fold axis. The subunit structure of eHspAT is shown with secondary structure assignments by the program DSSP (*32*) in Figure 4. A small domain is formed by two parts of the polypeptide chains from Tyr13 to Ala48 and from Ile326 to the C-terminus and the large domain from Val49 to Met325. The N-terminal part comprising Met1−Leu12 is called an arm and does not belong to either domain. The large domain is an α/β domain with an open twisted β-sheet structure. The seven β-strands designated a, g, f, e, d, b, and c (all parallel except for the g-strand) form a sharply twisted β-sheet structure as a central core surrounded by three α-helices (H5, H6, and H11) from the interior side of the protein and three α-helices (H3, H7, and H8) from the surface side (Figure 4). Many of the active-site residues are situated at or near one end of a seven-stranded β-sheet (the C-terminus of a-, f-, e-, d-, and b-strands and the N-terminus of the g-strand) forming the base of the active-site cavity. α-Helix H12 is located around the molecular 2-fold axis, and participates in the formation of the subunit interface. The small domain also assumes an α/β structure with a four-stranded-like β-sheet surrounded by three α-helices (H13, H15, and H16) from the surface side of the small domain. The antiparallel β-sheet of four strands (b″, b′, d′, and c′) is linked to the parallel β-sheet of two strands (c′ and a′) by sharing β-strand c′ to give the four-stranded-like β-sheet.

PLP-dependent enzymes have been classified into four families (fold type I−IV) (*33*), and the fold type I was subdivided into subgroups I−IV. The AspATs were assigned to the subgroup I (*17*), which was further subdivided into subgroups Ia and Ib (*18*). The program DALI (*31*) was used to search the Protein Data Bank database for PLP-dependent enzymes having a structure similar to that of eHspAT. The highest Z-scores (strength of structural similarity) were calculated to be 35.3 for tAspAT (*19*), 32.8 for tyrosine aminotransferase from *Trypanosoma cruzi* (*34*), 32.3 for cystalysin from *Treponema denticola* (*35*), 30.4 for the MalY protein from *E. coli* (*36*), 30.2 for aminocyclopropane 1-carboxylate synthase from *Malus domestica* (*37*), and 24.2 for cAspAT (*15*). Since the first four enzymes with the highest scores belong to subgroup Ib (*19*, *33*) and the sixth enzyme is a member of subgroup Ia, eHspAT might be assigned to subgroup Ib. More accurately, the overall structure of eHspAT is more similar to that of subgroup Ib than to subgroup Ia, because eHspAT shows relatively low Z-scores from 30.4 to 35.2 to the first four enzymes, compared with the Z-scores from 35.7 to 47.2 among these four enzymes.

Open-Closed Conformational Change. One of the striking features of the AspATs in subgroup Ia is the overall enzymatic conformational change from the open to the closed form, depending on the binding of the substrates (*10*−*15*). This conformational change is due to the small domain movement to close the active site. Also, in the tAspAT of subgroup Ib, the substrate binding induces a large conformational change from the open to the closed form. However, only the N-terminal region (Lys13−Val30) of the small domain approaches the active site to interact with the substrate (*19*).

The Cα atoms of the residues (5−17, 33−351) located on the electron density map of the native eHspAT were superimposed onto the corresponding atoms of eHspAT·Hsp and eHspAT·Pxy−Glu by least-squares fitting with rms deviations of 0.16 and 0.17 Å and maximum displacements of 0.75 and 0.60 Å, respectively, indicating that the enzyme does not change its main-chain folding of these residues upon binding with Hsp or glutamate. However, the structure of native eHspAT is distinguishable from those of eHspAT·Hsp and eHspAT·Pxy−Glu. The residues from 18 to 32 of the N-terminal region of the small domain were disordered in eHspAT, while the six residues (18−21, 31−32) in eHspAT·Hsp and the two residues (23, 24) showed their ordered structures. In eHspAT·Hsp, Thr18, Pro19, Tyr20, and Gln21 covered the active site. The binding substrate, Hsp, is almost shielded from the solvent, since the ASA of 375 Å^2 in Hsp is reduced to 13.0 Å^2. In tAspAT, the N-terminal region from Lys13 to Val30 moves to close the active site, while the enzyme, except for this mobile region, keeps their main-chain folding. Thus, eHspAT exhibits an open-closed conformational change on binding of Hsp, and the behavior of the N-terminal regions of eHspAT mimics that of tAspAT in subgroup Ib. In eHspAT·Pxy−Glu, Ala23 and Arg24 approached the active site, and the ASA of 318 Å^2 in Glu is reduced to 34 Å^2. But, the γ-carboxylate of Glu is exposed to the solvent region with the ASA of 25 Å^2.

Active Site of eHspAT in PLP form. The stereo structure and hydrogen-bonding scheme of the active site are shown in Figures 6a and 7a, respectively. The molecule has two active-site pockets around the molecular 2-fold axis. Each pocket is located at the domain interface of one subunit and at the subunit interface. The residues comprising the pocket are made up of two parts. The first part is the bottom of the active-site pocket, which consists of the residues, Asn194 (Asn in tAspAT and eAspAT), Asp222 (Asp), Ala224 (Ile and Ala), Tyr225 (Tyr), Thr255 (Gly and Ser), Ser257 (Ala and Ser), and Lys258 (Lys) and is at one end of the seven-stranded β-sheet of the large domain. The second part forms the active-site wall, and consists of Ala37 (Ala and Ile), Asp109 (Lys and Thr), Tyr140 (Trp), Arg382 (Val), Arg386 (Arg), Tyr70* (Tyr), and Tyr296* (Thr and Ser). Seven and eight residues of the active-site pocket are conserved between eHspAT, and tAspAT of subgroup Ib (*19*) and eAspAT of subgroup Ia (*12*−*14*), respectively, indicating a higher conservation of the active-site residues than those of other parts of the molecule. The corresponding α-carbons of the active-site residues are superposed by a least-squares method between eHspAT, and tAspAT and eAspAT. The Cα atoms of the active-site residues of eHspAT fit the corresponding atoms in tAspAT with an rms deviation of 1.74 Å. The rms deviation of the Cα atoms between eHspAT and eAspAT is 1.46 Å. When the Cα atoms of four residues (sequence number 37, 296, 382, and 386) are excluded from the least-squares fitting, the corresponding rms deviations between eHspAT, and tAspAT and eAspAT are 0.66 and 0.54 Å, respectively. These results indicate that the folding of the active-site residues are similar among these three enzymes, but Cα atoms of Ala37, Tyr296*, Arg382, and Arg386 are significantly displaced compared with those in tAspAT and eAspAT.

PLP is bound to this pocket by extensive noncovalent interactions with the residues forming the base of the active-site pocket except for Tyr70* and by forming an internal aldimine bond (Schiff base linkage) with the catalytic residue Lys258. The pyridine ring of PLP is sandwiched by the methyl group of Ala224 (the ethyl group of Ile in tAspAT and the methyl group of Ala in eAspAT) and the hydroxyphenyl ring of Tyr140 (the indole ring of Trp in tAspAT and eAspAT). The pyridine ring of the cofactor makes an angle of 12.0° with the hydroxyphenyl ring of Tyr140, while in tAspAT and eAspAT, the corresponding angles between the pyridine and indole rings are 6.1° and 20°, respectively (*12*, *19*).

The phosphate group of PLP is involved in seven hydrogen bonds and acts as an anchor to fix the cofactor to the active site. The negative charge of the phosphate group is well balanced with the positive charge of Arg266 and the dipole of α-helix H5, whose N-terminus is close to the phosphate group. Asp222 forms an ion pair with the protonated nitrogen atom of the pyridine ring of PLP. Tyr225 and Asn194 are hydrogen bonded to O3$^-$ of PLP. Five water molecules are located in the active-site pocket and are involved in the formation of hydrogen bond networks as is shown in Figures 6a and 7a. W1, W2, W3, and W4 form a one-dimensional hydrogen bond network with a branch to W5. Asp109 bridges W1 and the OH of Tyr140. W2 and W3 are hydrogen bonded to the OH of Tyr70* and the main-chain C═O of Ala37, respectively. W4 bridges the guanidino groups of Arg382 and Arg386, relaxing the repulsive forces between them. Arg386 is further hydrogen bonded to Asn194 and the C═O of Asn36.

Active Site of eHspAT·Hsp. The $2F_o - F_c$ electron density map for the Hsp−cofactor complex and the residues around it is shown in Figure 5a. The stereo structure and hydrogen-bonding scheme of the active site in eHspAT·Hsp are shown in Figures 6b and 7b. The binding of Hsp liberates five water molecules (W1−W5) from the substrate binding region of the active site in the free enzyme, inducing residues Thr18, Pro19, Tyr20, Gln21, Gly31, and Asp32 to be ordered, and approach and close the active site. Upon binding of the substrate, the cofactor makes a new covalent bond with Hsp in place of Lys258. Possibly, the major component of the Hsp−cofactor bond structure is ketimine based on the solution spectra, crystal color, and the agreement between the substrate model and residual electron density (see Materials and Methods). The released amino group of Lys258 makes a hydrogen bond with Tyr70*, which will decrease the free energy level of the Hsp−cofactor complex form of the enzyme. New hydrogen bond network is formed between the Hsp and the surrounding residues. However, the active-site residues except for Lys258 do not change their positions and retain the interactions among them upon Hsp binding,

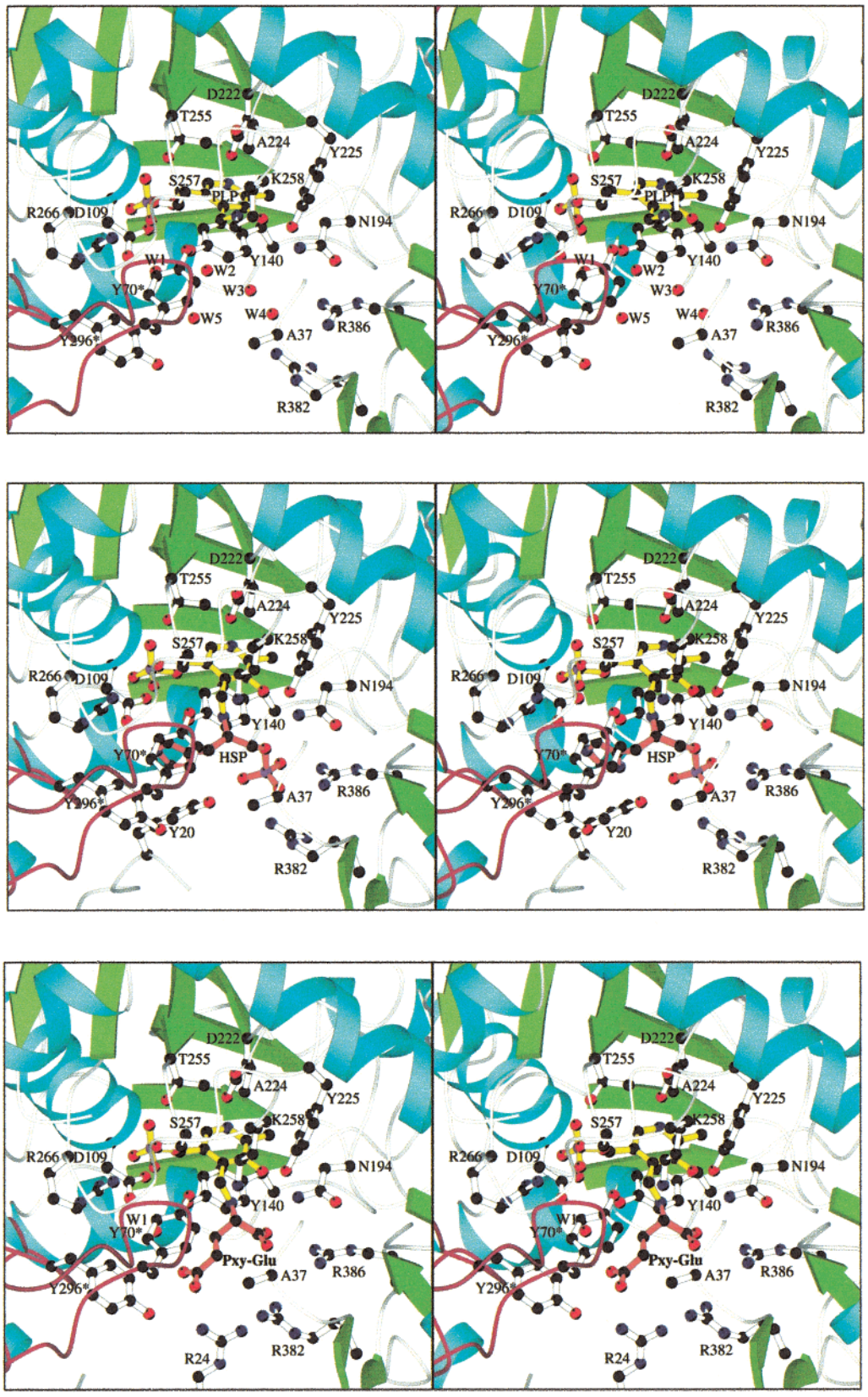

FIGURE 6: Stereoview of the active site in eHspAT. The upper and lower parts of each figure are the protein (bottom of the active site) and solvent (entrance of the active site) sides, respectively. (a, top) A close-up view of the active site of the unliganded eHspAT. Two loops (red) of the small domain of the other subunit participate in the formation of the active site. The active-site residues and PLP (yellow) are shown by a ball-and-stick model. The N-terminal region from Trp18 to Asp32 is missing because the region is disordered. (b, middle) Close-up view of the active site of eHspAT in complex with Hsp. Part of the missing region (the residues 18−21) in the unliganded form showed its ordered structure on the active-site pocket, and is displayed with Tyr20. Hsp is colored red with the cofactor in yellow. (c, bottom) Close-up view of the active site of eHspAT·Pxy−Glu. Glu is colored red with the cofactor in yellow. The γ-carboxylate of Glu directs toward the solvent side, and has weak interactions with Arg24 which is disordered in the unliganded enzyme.

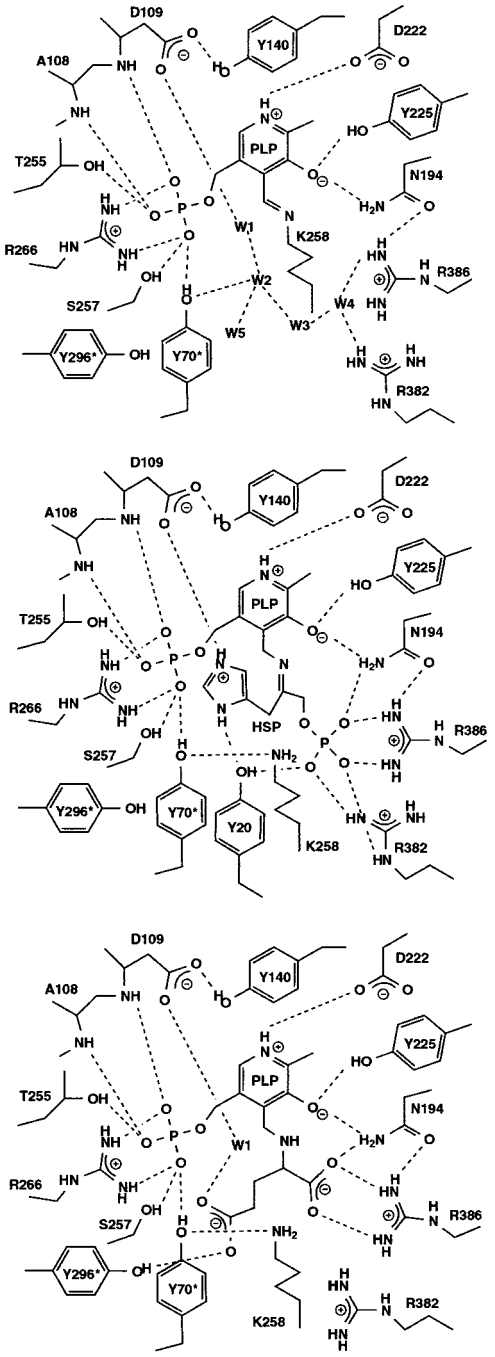

FIGURE 7: Schematic diagram showing hydrogen bond and salt bridge interactions of active-site residues in the unliganded eHspAT (a, top), eHspAT·Hsp (b, middle), and eHspAT·Pxy−Glu (c, bottom). Putative interactions are shown by dotted lines if the acceptor and donor are less than 3.5 Å apart.

since the corresponding residues in the free enzyme and the complex are superimposed within 0.21 Å with the maximum displacement of 0.483 Å except for the side chain of Lys258. The N-terminal residue Tyr20 covers the entrance of the active-site pocket to shield Hsp from the solvent.

The imidazole group of Hsp takes the place of W1 and W2 to form hydrogen bonds with Asp109 and Tyr20. The phosphate group of Hsp occupies the positions of W3 and W4, and makes salt bridges with Arg 382 and Arg386, and hydrogen bonds with Tyr20 and Asn194. The pyridine ring of the cofactor and the hydroxyphenyl ring of Tyr140 both rotate by 13° and 10° toward the solvent side, respectively, compared with those in the free enzyme. This rotation is induced by the formation of a covalent bond between the cofactor and Hsp, which are fixed at the substrate binding site by extensive interactions with the active-site residues. Also, in the tAspAT of subgroup Ib, a cooperative rotation (about 12°) of the cofactor and Trp140 was observed (*19*).

Active Site of eHspAT·Pxy−Glu. The $2F_o - F_c$ electron density map for Pxy−Glu and the residues around it is shown in Figure 5b. The stereo structure and hydrogen-bonding scheme of the active site in eHspAT·Pxy−Glu are shown in Figures 6c and 7c. Out of five water molecules located on the substrate binding region of the active-site in the free enzyme, four water molecules (W2−W5) are liberated, inducing the residues Ala23 and Arg24 to be ordered, and approach the active site. The amino group of Lys258 makes a hydrogen bond with Tyr70*. New hydrogen bond network is formed between the glutamate part of Pxy−Glu and the surrounding residues. However, the active-site residues except for Lys258 and Arg382 do not change their positions and retain the interactions among them upon glutamate binding, since the corresponding residues in the free enzyme and the complex are superimposed within 0.25 Å with the maximum displacement of 0.62 Å except for the side chains of Lys258 and Arg382.

The side chain of the glutamate part in Pxy−Glu takes the place of W2 and W5 to form hydrogen bonds with W1 and Tyr296*. The α-carboxylate group of the glutamate part occupies the positions of W3 and W4, and makes a salt bridge with Arg386, and a hydrogen bond with Asn194. The pyridine ring of the cofactor and the hydroxyphenyl ring of Tyr140 both rotate by 17° and 8° toward the solvent side, respectively, compared with those in the free enzyme.

Substrate Recognition. The eHspAT recognizes the substrates Hsp and glutamate, which are different in size, shape, charge, and property, using the same active site. The mechanism for the double substrate recognition in eHspAT has now been uncovered.

In eHspAT·Hsp, the phosphate group of Hsp is recognized by Arg382, Arg386, Tyr20, and Asn194 (Figures 6b and 7b). Arg382 and Arg386 form salt bridges/hydrogen bonds by side on and end on configurations, respectively (*38*), and the total two positive charges compensate the two negative charge of the phosphate group. Tyr20 and Asn194 interact with the phosphate group of Hsp as hydrogen bond donors. The imidazole group of Hsp is bound to the pocket constructed by the side chains of Tyr20, Tyr70*, Asp109, and Tyr296* (Figures 6b and 7b). Tyr20 and Asp109 are involved in the hydrogen bonds with the imidazole ring as hydrogen bond acceptors, implying that the imidazole ring is protonated. Tyr70* and Tyr296* make van der Waals contact with the imidazole ring.

In eHspAT·Pxy−Glu, The α-carboxylate group of glutamate is recognized by Arg386 and Asn194 (Figures 6c and 7c). The hydrogen bond network formed among Pxy−Glu, Arg386 and Asn194 is the same as that observed in the active site of eHspAT·Hsp. This network is common structural unit seen in aminotransferases of subgroup Ia and Ib (*9*−*15*, *19*). The acidic side-chain of glutamate forms hydrogen bonds with the hydroxy group of Tyr296* and W1 which is further hydrogen bonded to the carboxylate group of Asp109 (Figures 6c and 7c). Tyr70* makes a van der Waals contact with the side chain of glutamate. The residues (Tyr20, Tyr70,

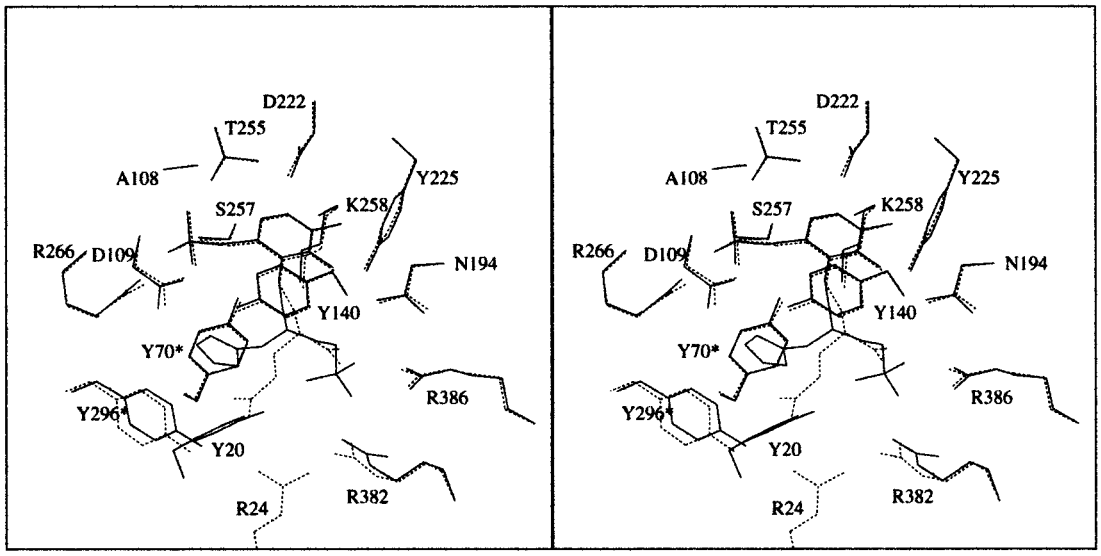

FIGURE 8: Superimposition of the active-site residues between eHspAT·Hsp and eHspAT·Pxy−Glu by least-squares fitting of all atoms except for Arg382 and Tyr296*. The active-site residues are well overlapped except for Arg382 and Tyr296*. Tyr20 and Arg24 are disordered in eHspAT·Hsp and eHspAT·Pxy−Glu, respectively. The imidazole ring of Hsp and γ-carboxylate of glutamate are located on the different positions of the active site.

Asp109, Asn194, Tyr296, Arg382, and Arg386) interacting with Hsp and/or glutamate are conserved in the HspATs, whose primary sequences have more than 34% sequence identities with eHspAT, and might interact with Hsp or glutamate in a mode similar to that observed in eHspAT·Hsp or eHspAT·Pxy−Glu.

The superposition of the active site between eHspAT·Hsp and eHspAT·Pxy−Glu is shown in Figure 8. The corresponding residues in eHspAT·Hsp and eHspAT·Pxy−Glu are superimposed within an rms deviation of 0.16 Å and the maximum displacement of 0.39 Å except for the side chains of Arg382 and Tyr296*, indicating that eHspAT recognizes both Hsp and glutamate without the large-scale rearrangement of the hydrogen bond networks and the active-site residues. A comparison of the location of Hsp in eHspAT·Hsp with that of glutamate in eHspAT·Pxy−Glu showed that the phosphate group of Hsp occupies the similar position as that of the α-carboxylate group of glutamate, while the basic imidazole group of Hsp and the acidic side chain of glutamte are located on the different positions showing that the binding site for the basic imidazole group of Hsp is different from that for the acidic side chain of glutamate (Figure 8). The bulky phosphate group of Hsp is folded to make short hydrogen bonds (2.7 and 2.8 Å) with the guanidino group of Arg386 compared with the corresponding ones (3.0 and 3.3 Å) in eHspAT·Pxy−Glu. The imidazole group of Hsp faces the protein side and is shielded from the solvent region. On the other hand, the acidic side chain of glutamate is directed to the opposite side and approach the solvent region. The mechanism for the double substrate recognition observed in eHspAT is in contrast to that in the hexamutant of eAspAT and an aromatic amino acid aminotransferase (*2*, *3*). In these enzymes, the recognition site for the side chain of the acidic amino acid is formed at the same position as that for the side chain of the aromatic amino acids by large-scale rearrangements of the hydrogen bond networks. This position is quite similar to that for the recognition site for the imidazole group of Hsp in eHspAT·Hsp and that for the acidic side chain of aspartate or glutamate in AspATs (*11*−*15*, *19*, *39*). Interestingly, AspATs and eHspAT homologous to AspATs bind the acidic side chains at the different locations of the active site.

Among the residues interacting with Hsp and/or glutamate, Tyr70*, Asn194, and Arg386 are conserved in the AspATs and have common roles in eHspAT and the AspATs. In the AspATs, Tyr70* approaches the side-chain of the substrate (*9*-*15*), and Asn194 and Arg386 interact with the α-carboxylate in the same manner as observed in eHspAT·Hsp and eHspAT·glutamate. Thus, the unconserved residues, Tyr20, Asp109, Tyr296*, and Arg382 are characteristic of the Hsp and/or glutamate recognition.

In eHspAT·Hsp, the disordered Tyr20 in the free enzyme approaches Hsp, bridges the imidazole ring and the phosphate group by hydrogen bonds, and almost shields Hsp from the solvent. The induced fit of the N-terminal region bearing Tyr20 is critical for Hsp recognition. Asp109 induces the protonation of the imidazole ring, and forms a strong hydrogen bond with the ring. In tAspAT of subgroup Ib, the residue 109 is Lys, which is a key residue to recognize the side-chain carboxylate (*19*), while in subgroup Ia AspAT, Arg292 takes the place of Lys109 to interact with the side chain of the substrate (*9*−*15*). Asp109 in eHspAT and Lys109 in tAspAT play a role similar in the substrate recognition, although their charges are opposite. Tyr296* participates in the formation of the pocket for the imidazole ring of Hsp, directly interacting with the ring. Thus, Tyr20, Asp109, and Tyr296* are key residues to recognize the imidazole group of Hsp. Most of the residues 382 in AspATs are hydrophobic Ile, Leu, or Val, which are situated just on Arg386. In eHspAT, the residue is replaced by Arg to interact with the phosphate group of the substrate. Arg382 is one of the key residues for substrate recognition.

In eHspAT·glutamate, the binding of the substrate glutamate induces the approach of the disordered loop toward the active site. But the behavior of the loop is different from that of eHspAT·Hsp in that Arg24 shows its ordered structure with Tyr20 disordered. Arg382 changes its side-chain direction to approach the γ-carboxylate of glutamate. The distances

between the guanidino groups of Arg24 and Arg382, and the γ-carboxylate are 5.6 and 4.8 Å, respectively. The two Arg residues may at least partially compensate the negative charge of the γ-carboxylate by the electrostatic interactions. Asp109 and Tyr296* participate in the recognition not only for the imidazole group of Hsp in eHspAT·Hsp but also for the γ-carboxylate of glutamate. Asp109 interacts with the γ-carboxylate of glutamate in the medium of W1 and Tyr296* makes a direct hydrogen bond with the γ-carboxylate.

The eHspAT, tAspAT, and eAspAT are divergently evolved from the same ancestor. eHspAT gained the ability to recognize both Hsp and glutamate and catalyze them, by utilizing essentially the same active-site folding as that of AspAT, conserving the essential residues for transamination reaction, and replacing and relocating some of the active-site residues to make the binding sites for the phosphate and the α-carboxylate groups of the substrates at the same position and those for the imidazole and γ-carboxylate groups at the different positions.

Mechanistic Implications. Comparison of the active-site residues of eHspAT described above with those of the AspATs of subgroup Ia and tAspAT of subgroup Ib showed that the essential residues for the catalytic actions in the AspATs are conserved in eHspAT. These residues are Asn194, Asp222, Tyr225, and Lys258. Asn194, Tyr225, and Asp222 control the electronic state of the π-conjugate system of the Hsp−cofactor bond structure through hydrogen bonds to $O3^-$ and a salt bridge to $N1^+$ of the cofactor (*40*-*43*), and Lys258 is the catalytic residue as a proton shuttle. In addition to these residues, Tyr70 and Arg386 are conserved. Tyr70 makes a van der Waals contact with the side chain of the substrate (*44*), and Arg386 recognizes the α-carboxylate of the substrate (*9*-*15*). The main-chain atoms of the conserved residues except for Arg386 are superimposed within 0.87 Å with those of eAspAT of subgroup Ia, and the locations of the side chains of these residues are approximately the same between eHspAT and eAspAT, indicating that the stereochemistry of the catalytic reaction in eHspAT is the same as those proposed for the AspATs of subgroup Ia (*7*).

In the uncomplexed AspATs of subgroup Ia in the PLP form, the Schiff base (C4′═N) between PLP and Lys258 was characterized by the unusually low pK_a value of about 6.8, and the large deviation of the C4′═N bond from the planar π-conjugated system between C4′═N and the pyridine ring of PLP with the dihedral angle of C3−C4−C4′−N amounting to 50−90° (*12*−*15*). The deviation of C4′═N and the low pK_a value were proved to be caused by the stereochemical strain of the protonated Schiff base coplanar with the pyridine ring of PLP: the Schiff base is tethered to the protein backbone, and the rotation of the pyridine ring of PLP is restricted by the access of Ala224 (*43*, *45*). This strain is essential for the enzyme function, since the strain of the protonated Schiff base enhances the catalytic activity of the enzyme by increasing the energy level of the free enzyme plus substrate at a neutral pH relative to the transition state (*45*). Also, in eHspAT, the Schiff base formed by PLP and Lys258 deviate significantly from the plane of the pyridine ring of PLP with the dihedral angle of C3−C4−C4′−N = 52°. The Schiff base is linked to the protein backbone, and the rotation of the pyridine ring of PLP is restricted by Ala224, with the active-site structure around PLP similar to that of the AspAT subgroup Ia, suggesting that the strain of the protonated Schiff base is critical for the catalytic action of this enzyme. This hypothesis is now being tested by mutational analysis.

REFERENCES

1. Christen, P., and Metzler, D. E., Eds. (1985) *Transaminases*, J. Wiley and Sons, New York.
2. Malashkevich, V. N., Onuffer, J. J., Kirsch, J. F., and Jansonius, J. N. (1995) *Nat. Struct. Biol. 2*, 548−553.
3. Okamoto, A., Nakai, Y., Hayashi, H., Hirotsu, K., and Kagamiyama, H. (1998) *J. Mol. Biol.* 280, 443−461.
4. Martin, R. G., Berberich, M. A., Ames, B. N., Davis, W. W., Goldberger, R. F., and Yourno, J. D. (1971) *Methods Enzymol. 17B*, 3−44.
5. Grisolia, V., Carlomagno, M. S., Nappo, A. G., and Btuni, C. B. (1985) *J. Bacteriol. 164*, 1317−1323.
6. Karpeisky, M. Y., and Ivanov V. I. (1966) *Nature 210*, 493−496.
7. Kirsch, J. F., Eichele, G., Ford, G. C., Vincent, M. G., Jansonius, J. N., Gehring, H., and Christen, P. (1984) *J. Mol. Biol. 174*, 3497−3525.
8. Mehta, P. K., Hale, T. I., and Christen, P. (1989) *Eur. J. Biochem. 186*, 249−253.
9. Jansonius, J. N., and Vincent, M. G. (1987) *Structural basis for catalysis by aspartate aminotransferase in biological macromolecules and assemblies* (Jurnak, F. A., and Mcpherson, A., Eds.) pp 187−285, J. Wiley and Sons, New York.
10. McPhalen, C. A., Vincent, M. G., and Jansonius, J. N. (1992) *J. Mol. Biol. 225*, 495−517.
11. Malashkevich, V. N., Strokopytov, B. V., Borisov, V. V., Dauter, Z., Wilson, K. S., and Torchinsky, Y. M. (1995) *J. Mol. Biol. 247*, 111−124.
12. Okamoto, A., Higuchi, T., Hirotsu, K., Kuramitsu, S., and Kagamiyama, H. (1994) *J. Biochem. 116*, 95−107.
13. Jäger. J., Moser, M., Sauder, U., and Jansonius. J. N. (1994) *J. Mol. Biol. 239*, 285−305.
14. Miyahara, I., Hirotsu, K., Hayashi, H., and Kagamiyama, H. (1994) *J. Biochem. 116*, 1001−1012.
15. Rhee, S., Silva, M. M., Hyde, C. C., Rogers, P. H., Metzler, C. M., Metzler, D. E., and Arnone, A. (1997) *J. Biol. Chem. 272*, 17293−17302.
16. Jansonius, J. N. (1998) *Curr. Opin. Struct. Biol. 8*, 759−769.
17. Mehta, P. K., Hale, T. I., and Christen, P. (1993) *Eur. J. Biochem. 214*, 549−561.
18. Okamoto, A., Kato, R., Masui, R., Yamagishi, A., Oshima, T., and Kuramitsu, S. (1996) *J. Biochem. 119*, 135−144.
19. Nakai, T., Okada, K., Akutsu, S., Miyahara, I., Kawaguchi, S., Kato, R., Kuramitsu, S., and Hirotsu, K. (1999) *Biochemistry 38*, 2413−2424.
20. Thompson, J. D., Higgins, D. G., and Gibson T. J. (1994) *Nucleic Acids Res. 22*, 4673−4680.
21. Severin, E. S., Gulyaev, N. N., Khurs, E. N., and Khomutov, R. M. (1969) *Biochem. Biophys. Res. Commun. 35*, 318−323.
22. Hendrickson, W. A., Horton, J. R., and LeMaster, D. M. (1990) *EMBO J. 9*, 1665−1672.
23. Otwinowski, Z. (1993) Data collection and processing. In *Proceedings of the CCP4 Study Weekend*, pp 56−62, SERC Daresbury Laboratory, Warrington.
24. Collaborative Computational Project Number 4 (1994) *Acta Crystallogr., Sect. D 50*, 760−763.
25. Wang, B.-C. (1985) *Methods Enzymol. 115*, 90−112.
26. Zhang, K. Y. J., and Main, P. (1990) *Acta Crystallogr., Sect. A 46*, 377−381.
27. Jones, T. A., Zou, J.-Y., Cowan, S. W., and Kjeldgaard, M. (1991) *Acta Crystallogr., Sect. A 47*, 110−119.
28. Brünger, A. T., Kuriyan, J., and Karplus, M. (1987) *Science 235*, 458−460.
29. Brünger, A. T. (1991) *Annu. Rev. Phys. Chem. 42*, 197−223.

30. Laskowski, R. A., MacArthur, M. W., Moss, D. S., and Thornton, J. M. (1993) *J. Appl. Crystallogr. 26*, 283−291.
31. Holm, L., and Sander, C. (1993) *J. Mol. Biol. 233*, 123−138.
32. Kabsch, W., and Sander, C. (1983) *Biopolymers 22*, 2577−2637.
33. Grishin, N. V., Phillips, M. A., and Goldsmith, E. J. (1995) *Protein Sci. 4*, 1291−304.
34. Blankenfeldt, W., Nowicki, C., Montemartini-Kalisz, M., Kalisz, H. M., and Hecht, H. J. (1999) *Protein Sci. 8*, 2406−2417.
35. Krupka, H. I., Huber, R., Holt, S. C., and Clausen, T. (2000) *EMBO J. 19*, 3168−3178.
36. Clausen, T., Schlegel, A., Peist, R., Schneider, E., Steegborn, C., Chang, Y. S., Haase, A., Bourenkov, G. P., Bartunik, H. D., and Boos, W. (2000) *EMBO J. 19*, 831−842.
37. Capitani, G., Hohenester, E., Feng, L., Storici, P., Kirsch, J. F., and Jansonius J. N. (1999) *J. Mol. Biol. 294*, 745−756.
38. Mitchell, J. B., Thornton, J. M., Singh, J., and Price, S. L. (1992) *J. Mol. Biol. 226*, 251−262.
39. Malashkevich, V. N., Toney, M. D., and Janonius, J. N. (1993) *Biochemistry 32*, 13451−13462.
40. Inoue, K., Kuramitsu, S., Okamoto, A., Hirotsu, K., Higuchi, T., Morino, Y., and Kagamiyama, H. (1991) *J. Biochem. 109*, 570−576.
41. Yano, T., Kuramitsu, S., Tanase, S., Morino, Y., and Kagamiyama, H. (1992) *Biochemistry 31*, 5878−5887.
42. Yano, T., Hinoue, Y., Chen, V. J., Metzler, D. E., Miyahara, I., Hirotsu, K., and Kagamiyama, H. (1993) *J. Mol. Biol. 234*, 1218−1229.
43. Hayashi, H. (1995) Pyridoxal enzymes: mechanistic diversity and uniformity. *J. Biochem. 118*, 463−473.
44. Inoue, K., Kuramitsu, S., Okamoto, A., Hirotsu, K., Higuchi, T., and Kagamiyama, H. (1991) *Biochemistry* 30, 7796−7801.
45. Hayashi, H., Mizuguchi, H., and Kagamiyama, H. (1998) *Biochemistry 37*, 15076−15085.

BI002769U